GA–A22788

CONF-971103--

EXPERIMENTAL CONSTRAINTS ON TRANSPORT FROM DIMENSIONLESS PARAMETER SCALING STUDIES

by

C.C. PETTY, T.C. LUCE, D.R. BAKER, B. BALLET,
T.N. CARLSTROM, J.G. CORDEY, J.C. DE BOO,
P. GOHIL, R.J. GROEBNER, B.W. RICE,
D.M. THOMAS, M.R. WADE, and R.E. WALTZ

FEBRUARY 1998

GENERAL ATOMICS

DISCLAIMER

GA–A22788

EXPERIMENTAL CONSTRAINTS ON TRANSPORT FROM DIMENSIONLESS PARAMETER SCALING STUDIES

by

C.C. PETTY, T.C. LUCE, D.R. BAKER, B. BALLET,[1]
T.N. CARLSTROM, J.G. CORDEY,[1] J.C. DE BOO,
P. GOHIL, R.J. GROEBNER, B.W. RICE,[2]
D.M. THOMAS, M.R. WADE,[3] and R.E. WALTZ

This is a preprint of an invited paper presented at the 39th Annual Meeting of the Division of Plasma Physics, American Physical Society, November 17–21, 1997, Pittsburgh, Pennsylvania, and to be printed in a Special Issue of *Physics of Plasmas.*

Work supported by U.S. Department of Energy
under Contracts DE-AC03-89ER51114,
W-7405-ENG-48, and DE-AC05-96OR22464

[1]Jet Joint Undertaking
[2]Lawrence Livermore National Laboratory
[3]Oak Ridge National Laboratory

GENERAL ATOMICS PROJECT 3466
FEBRUARY 1997

Experimental constraints on transport from dimensionless parameter scaling studies

C.C. Petty,[a] T.C. Luce, D.R. Baker, B. Ballet,[b] T.N. Carlstrom, J.G. Cordey,[b] J.C. DeBoo, P. Gohil, R.J. Groebner, B.W. Rice,[c] D.M. Thomas, M.R. Wade,[d] and R.E. Waltz

General Atomics, P.O. Box 85608
San Diego, California 92186-5608 U.S.A.

Abstract

The scalings of heat transport with safety factor (q), normalized collisionality (ν), plasma beta (β), and relative gyroradius (ρ_*) have been measured on the DIII–D tokamak [Fusion Technol. 8, 441 (1985)]. The measured ρ_*, β and ν scalings of heat transport indicate that $E \times B$ transport from drift wave turbulence is a plausible basis for anomalous transport. For high confinement (H) mode plasmas where the safety factor was varied at fixed magnetic shear, the effective (or one-fluid) thermal diffusivity was found to scale like $\chi_{\text{eff}} \propto q^{2.3\pm0.64}$, with the ion and electron fluids having the same q scaling to within the experimental errors except near the plasma edge. The scaling of the thermal confinement time with safety factor was in good agreement with this local transport dependence, $\tau_{\text{th}} \propto q^{-2.42\pm0.31}$; however, when the magnetic shear was allowed to vary to keep q_0 fixed during the (edge) safety factor scan, a weaker global dependence was observed, $\tau_{\text{th}} \propto q_{95}^{-1.43\pm0.23}$. This weaker dependence was mainly due to the change in the local value of q between the two types of scans. The combined ρ_*, β, ν and q scalings of heat transport for H–mode plasmas on DIII–D reproduce the empirical confinement scaling using physical (dimensionless) parameters with the exception of weaker power degradation.

---

[a] Invited speaker.
[b] JET Joint Undertaking, Abingdon, Oxfordshire, U.K.
[c] Lawrence Livermore National Laboratory, Livermore, California, U.S.A.
[d] Oak Ridge National Laboratory, Oak Ridge, Tennessee, U.S.A.

I. Introduction

The related methods of dimensional analysis, similarity, and scale invariance in physics provide a powerful technique for analyzing physical systems.[1,2] Significant progress has been made recently towards predicting and understanding radial heat transport using dimensionless parameter scaling techniques. Most of the dimensionless parameter scaling experiments to date have concentrated on measuring the relative gyroradius (ρ_*) scaling of heat transport,[3–10] although the beta (β) scaling[8,11–13] and collisionality (ν) scaling[8,11,13,14] have also been reported. In this paper, the results from a ''proof-of-principle'' test of the dimensionless parameter scaling approach to transport studies are reported, where the energy confinement is compared for discharges on DIII–D[15] and the Joint European Torus[16] (JET) that had identical values for all of the relevant dimensionless quantities. In addition, the safety factor scaling of heat transport is measured for the first time with all the dimensionless quantities held fixed, including the magnetic shear. Experimentally determining these dimensionless parameter scalings helps to distinguish between various proposed instability mechanisms of turbulent transport and permits the confinement properties of future magnetic fusion devices to be extrapolated from existing experiments.

If radial heat transport is governed only by plasma physics (*i.e.*, the Boltzmann and Maxwell equations), then Connor-Taylor scale invariance arguments[2] lead to a thermal diffusivity (χ) that is dependent only upon the local dimensionless quantities,

$$\frac{\chi}{\chi_B} = F\left(q, \rho_*, \beta, \nu, \frac{T_e}{T_i}, \varepsilon, \kappa, \ldots\right). \tag{1}$$

In this equation, $\chi_B \sim T/eB$ is the Bohm diffusion coefficient, $q = \varepsilon B_T / B_p \sim aB/I$ is the safety factor, $\rho_* \sim \sqrt{T}/aB$, $\beta \sim nT/B^2$, $\nu \sim na/T^2$, R is the plasma major radius, a is the plasma minor radius, ε is the inverse aspect ratio, κ is the plasma elongation, n is the plasma density, T is the plasma temperature, B is the magnetic field strength, and I is the plasma current. Dimensionless parameter scaling studies usually assume that the transport dependencies on the various dimensionless quantities can be represented as a power law scaling. For example, in an experiment to determine the safety factor scaling of confinement, it is assumed that Eq. (1) can be written in the form

$$\frac{\chi}{\chi_B} = q^{\alpha_q} G\left(\rho_*, \beta, \nu, \frac{T_e}{T_i}, \varepsilon, \kappa, \ldots\right). \tag{2}$$

Although this type of power law dependence is not general, experimentally it is difficult to determine a more complicated scaling, and it is convenient for later comparison with

empirically-derived confinement scaling relations based upon physical parameters. In this example, varying the safety factor while keeping the other dimensionless quantities (ρ_*, β, ν, ε, κ, *etc.*) fixed allows the exponent α_q to be determined from the measured change in the thermal diffusivity since the unknown function G remains constant.

The rest of this paper is organized as follows: in Section II, the proof-of-principle experiment of Eq. (1) on DIII–D and JET is discussed. Results from the safety factor scaling experiments in high confinement (H) mode plasmas on DIII–D are reported in Section III. In Section IV, the results and implications of gyroradius, beta, and collisionality scaling experiments on DIII–D in H–mode plasmas are discussed. A comparison of the DIII–D dimensionless parameter scaling studies with the physical parameter scalings from multi-machine confinement databases is given in Section V, while the conclusions are presented in Section VI. For these experiments on the DIII–D tokamak, single-null divertor plasmas are used with a plasma shape that is approximately the same as the expected shape for the International Thermonuclear Experimental Reactor[17] (ITER). Deuterium neutral beam injection (NBI) was used for auxiliary heating. The primary ion species was deuterium, with carbon being the dominant impurity species. The plasma diagnostics are described in Ref. 9.

II. Dimensionally Identical Discharges

A basic assumption of the dimensionless parameter scaling approach is that transport is dependent only upon local quantities. Therefore, if two plasmas with widely different physical parameters (*e.g.*, B and a) are constructed that have the same values for all of the dimensionless parameters in Eq. (1), then the thermal diffusivities normalized to the Bohm diffusion coefficient should also be the same for these two plasmas. Testing this assertion is an important proof-of-principle experiment for this approach to transport studies. Plasmas which have the same values for all of the dimensionless parameters are referred to as dimensionally identical discharges.

Experiments on DIII–D and JET have been done to compare the confinement of dimensionally identical discharges in H–mode plasmas with edge localized modes (ELMs). The global normalized plasma parameters and plasma shape were well matched, as shown in Table I. The inverse aspect ratio and elongation were the same to about 3%. In order to keep the globally averaged values of ρ_*, β, ν, and q fixed for these two plasmas with different B and a, the quantities $Ba^{5/4}$, $W_{\rm th}/a^{1/2}$, $\bar{n}a^2$, and $Ia^{1/4}$ were held constant. The experimental match to these global dimensionless parameters was better than 4% except for the normalized density (15% mismatch). Table I shows that the normalized thermal confinement times ($B\tau_{\rm th}$), with the NBI power corrected for shinethrough losses, agree to within about 7% for the DIII–D and JET dimensionally identical discharges, which was within the experimental uncertainties. Thus, plasmas that have identical values for the dimensionless parameters have been found to have the same (normalized) confinement, which demonstrates that dimensionless parameter scaling is a valid approach to understanding transport processes.

Table I: Global physical and dimensionless parameters for DIII–D and JET dimensionally identical H–mode discharges.

Parameter	DIII–D #86209	JET #33465
B (T)	2.15	1.07
R (m)	1.64	2.88
a (m)	0.55	0.95
I (MA)	1.19	1.04
$\bar{n}$ (10^{19} m^{-3})	7.7	3.1
W_{th} (MJ)	0.67	0.85
P (MW)	4.8	2.8
τ_{th} (s)	0.14	0.30
ε	0.34	0.33
κ	1.69	1.64
$Ba^{5/4}$	1.02	1.00
$W_{th} / a^{1/2}$	0.90	0.87
$\bar{n}a^2$	2.4	2.8
$Ia^{1/4}$	1.03	1.03
$B\tau_{th}$	0.30	0.32

III. Safety Factor Scaling of H–mode Confinement

The safety factor scalings of the energy confinement time and local thermal diffusivities were determined on DIII–D for H–mode plasmas by varying the plasma current at constant ρ_*, β, and ν. Although many tokamak experiments have measured the I scaling of confinement, this is usually done at fixed auxiliary heating power such that ρ_*, β, and ν are not held constant. Furthermore, since the safety factor on axis is typically fixed to a value near 1 by sawteeth, plasma current scans normally vary the local values of both the safety factor and the magnetic shear, $\hat{s} \equiv r\nabla q / q$, complicating the interpretation. Transport experiments in discharges with fast current ramps to provide a transient modification of the current profile have shown that local decreases in the thermal diffusivity were correlated with local increases in both the poloidal magnetic field and the magnetic shear.[18]

In these experiments, the safety factor scan was done in two ways: (1) a q scan at fixed $\hat{s}$, and (2) a combined q and $\hat{s}$ scan at fixed q_0. The first method allows the safety factor scaling of heat transport to be unambiguously determined, while the second method allows the magnetic shear dependence to be investigated and makes contact with the normal way that plasma current scans are done. In order to keep ρ_*, β, and ν constant during the safety factor scan, the plasma density, temperature and magnetic field strength were held fixed (if the plasma radius were to vary, then the quantities $Ba^{5/4}$, na^2, and $Ta^{1/2}$ would need to be held fixed). This means that the Bohm diffusion coefficient does not change during the safety factor scan, and the values of the thermal diffusivity and confinement time do not need to be normalized to χ_B in order to interpret the results.

Drift wave models of turbulent transport[19] generally predict a dependence of transport on the safety factor in the range of $\chi \propto q^{1-2}$. For example, the toroidal ion temperature gradient (ITG) mode and collisionless trapped electron mode exhibit an approximately linear increase in transport with increasing safety factor,[20] while models of the resistive ballooning mode,[21] which is predicted to be important only in the plasma edge, have a transport scaling like $\chi \propto q^2$. The dependence of the heat transport on the magnetic shear is expected to be more complicated and non-monotonic. The application of gyro-Landau fluid (GLF) model equations for toroidal geometry to ITG turbulence shows that transport has a relative maximum for values of magnetic shear around $\hat{s} \sim 0.5$, shifting to larger $\hat{s}$ with finite Shafranov shift, with transport decreasing as the magnetic shear either increases (strong positive shear) or decreases (weak or negative shear) away from this value.[22] Finally, neoclassical heat transport has a safety factor dependence similar to that of turbulent transport for fixed ν,

$$\chi_{neo} \sim \chi_B \rho_* \nu q^2 \ . \qquad (3)$$

III.A. Fixed magnetic shear case

In order to scan q at fixed $\hat{s}$, the safety factor was varied by a constant multiplicative factor across its entire radial profile by scanning the plasma current by a factor-of-1.4 in ELMing H–mode plasmas. The magnetic shear was held fixed during the current scan by controlling the formation and evolution of the q profile during the initial phase of the discharge by adjusting the level and timing of the NBI heating.[23] The high-q end of the safety factor scan was limited by the appearance of resistive tearing modes, while the low-q end was limited by a change in the ELM behavior due to the nearness of the H–mode threshold. Since the plasma beta and inverse aspect ratio were held constant, the normalized beta $\beta_N \equiv \beta / (I / aB)$ varied during the safety factor scan because $\beta_N \propto \beta q / \varepsilon$. Although this results in the high-q discharges being in closer proximity to the beta limit than the low-q discharges, experiments on DIII–D have found no degradation in heat transport with increasing β or β_N.[12]

The global parameters were well matched for the two discharges that comprised the safety factor scan at fixed magnetic shear. Table II shows that the plasma shape (R, a, and κ) was held fixed to within 1%, although the triangularity was allowed to vary by a larger amount (4%) in order to adjust the amount of divertor cryopumping for density control. The plasma densities and thermal stored energies were matched to within 5%, such that ρ_*, β^{th}, and ν were also nearly matched. The profiles of the safety factor and magnetic shear for the two discharges in Table II are shown in Fig. 1 as a function of the normalized flux coordinate ρ. The motional Stark effect (MSE) diagnostic was critical for determining the q profile in these experiments.[24] The safety factor was varied across the entire plasma radius by close to a constant factor-of-1.4, thus the magnetic shear was nearly unchanged.

The thermal confinement time was found to have a strong safety factor dependence for these H–mode discharges in fair agreement with theoretical expectations. Although the q profile was slowly evolving in time over the analysis window due to the relaxation of the parallel electric field, the resistive skin time was much longer than the energy confinement time, thus $\dot{W}$ corrections to the transport analysis were negligible (on the order of 1%). Table II shows that the thermal confinement time had a factor-of-2.2 increase for a factor-of-1.4 decrease in the safety factor. Therefore, the thermal confinement for H–mode plasmas scaled like $\tau_{th} \propto q^{-2.42}$ for the case of fixed magnetic shear; the random error in the q scaling exponent is less than 0.31 while the systematic error is thought to be less than ± 0.03. (A detailed explanation of the random and systematic error analysis is given in the Appendix of Ref. 12.)

In addition to the close match in the global parameters shown in Table II, the local values of the plasma parameters were also kept nearly fixed during the safety factor scan. The radial profiles of the electron and ion temperature, the electron density and the effective ion charge are shown in Fig. 2. The largest mismatch was in the Z_{eff} profile, which

Table II: Physical and dimensionless parameters for H–mode safety-factor scaling experiment at fixed magnetic shear.

Parameter	#92128	#92113
I (MA)	1.00	1.39
B (T)	1.89	1.90
R (m)	1.685	1.671
a (m)	0.605	0.601
$\bar{n}$ (10^{19} m^{-3})	4.31	4.13
W_{th} (MJ)	0.59	0.60
P (MW)	9.47	4.30
τ_{th} (s)	0.063	0.139
ε	0.36	0.36
κ	1.84	1.84
δ	0.25	0.24
q_{95}	5.66	3.87
q_0	1.9	1.4
β^{th} (%)	1.44	1.44
β_N^{th}	1.65	1.19

systematically varied by 25% between the two H–mode discharges. There was also a 12% systematic mismatch in the T_e / T_i ratios, although the plasma beta was well matched locally (except near the plasma center). If confinement has a square-root dependence on either Z_{eff} or T_e / T_i, for example, then the apparent value of α_q could be skewed by 0.3 and 0.2 units, respectively. If the temperature profiles are being held near their marginal stability points by plasma turbulence, as suggested by ITG models, then the measured transport may be sensitive to imperfect matches in the plasma parameters. The uncertainty in the safety factor scaling in this case is best quantified by comparing the predictions of theory-based transport modeling to the experimental profiles.

A local transport analysis found a strong safety factor dependence of the thermal diffusivities across the entire plasma radius for H–mode plasmas, the magnitude of which agreed with the scaling of the global confinement time. The radial power balance analysis was done using the ONETWO[25] code assuming that the heat flux was purely diffusive. The ratio of the effective (or one-fluid) thermal diffusivities for the safety factor scan of Table II is shown in Fig. 3, where the effective thermal diffusivity is defined by

$$\chi_{eff} = \frac{n_e \chi_e + n_i \chi_i}{n_e + n_i} \quad . \tag{4}$$

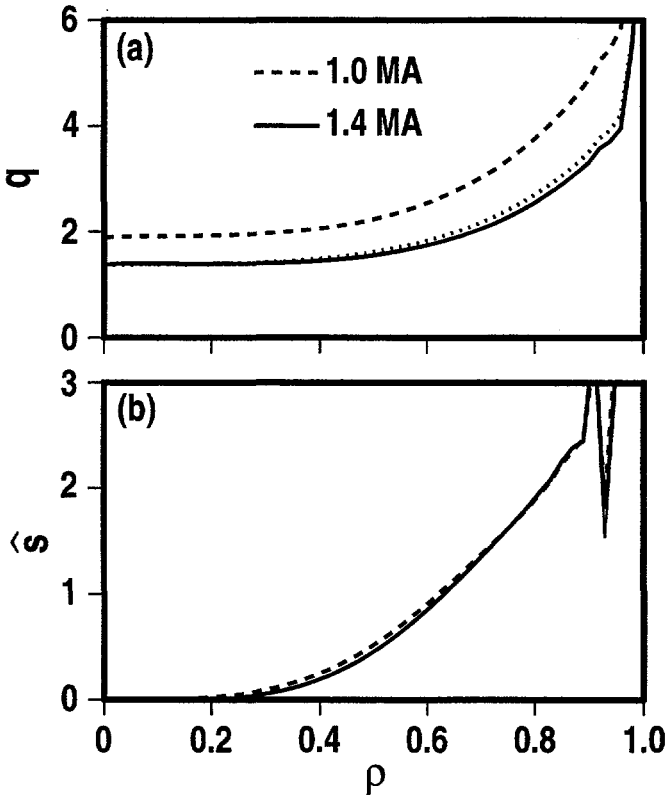

Fig. 1. Radial profiles of (a) safety factor, and (b) magnetic shear for the H–mode discharges in Table II. The dotted line in (a) represents the 1.0 MA profile scaled to 1.4 MA.

Transport results near the plasma center are not included in this figure due to the large experimental uncertainties in that region, while the edge region is excluded due to ELMs. Using Eq. (2), the safety factor scaling of the effective thermal diffusivity is found to be $\chi_{\text{eff}} \propto q^{2.3}$, with a random error of 0.64 and a systematic error of not more than ± 0.09 in the q scaling exponent.

A two-fluid transport analysis found that the electron and ion thermal diffusivities had the same dependence on safety factor to within the experimental errors over most of the plasma radius. This is demonstrated in Fig. 4, which shows the ratio of the ion and electron thermal diffusivities for the low-q and high-q H–mode discharges. The safety factor scaling of the ion fluid was nearly constant over the plasma radius and can be summarized as $\alpha_q = 2.5$ with a random error of 1.2 and a systematic error of not more than ± 0.35. The electron fluid exhibited a stronger radial variation in the safety factor scaling, the average value of which was $\alpha_q = 1.4$ with approximately the same uncertainties as for the ion fluid. The electron and ion dependencies on q were within one standard deviation of each other except near the plasma edge.

The strong safety factor scaling of the thermal diffusivity shown in Fig. 3 is in general agreement with theoretical predictions of drift wave models of turbulent transport.

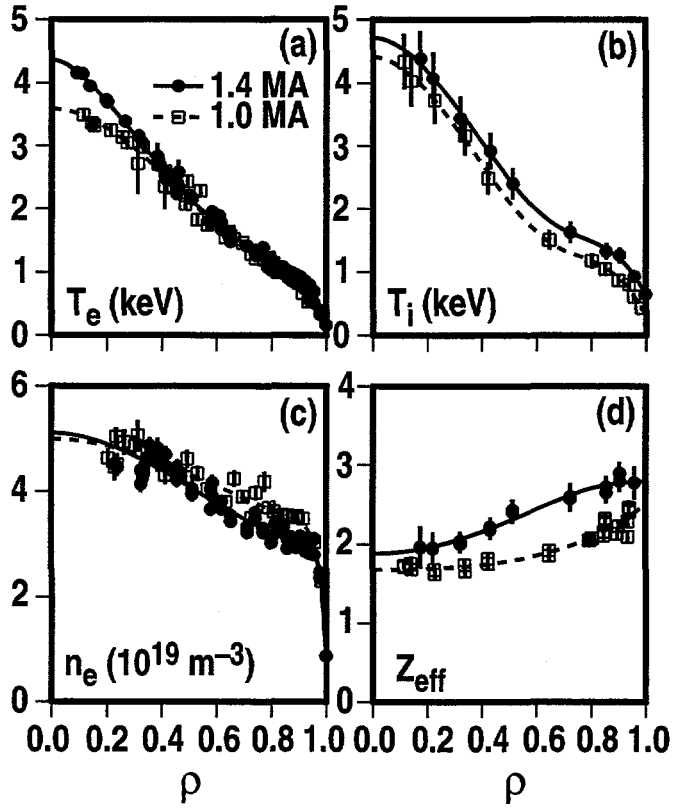

Fig. 2. Radial profiles of (a) electron temperature, (b) ion temperature, (c) electron density, and (d) effective ion charge for the H–mode discharges in Table II.

The measured transport dependence is close to $\chi_{eff} \sim q^2$ over much of the plasma radius, which is the expected scaling of the (edge) resistive ballooning mode and near the upper limit of the expected scaling for the toroidal ITG mode and collisionless trapped electron mode.[20] Before this q scaling can be compared to the empirically-derived physical parameter scaling relations, however, the dependence of transport on the magnetic shear needs to be investigated.

III.B. Fixed q_0 case

In the second part of this experiment, both the safety factor and magnetic shear were allowed to vary during the current scan so that q_0 was kept fixed. The other dimensionless parameters (ρ_*, β, ν) were held constant in the same way as for Section III.A. This combined q and $\hat{s}$ scan more closely resembles the usual way that I scaling of confinement is measured, and allows the dependence of heat transport on the magnetic shear to be studied. The value of q_0 was held fixed during the I scan by adjusting the level and timing of the NBI heating during the initial phase of the discharge.

The global parameters were well matched for the combined safety factor and magnetic shear scan in ELMing H–mode plasmas, as shown in Table III. The variations in the plasma

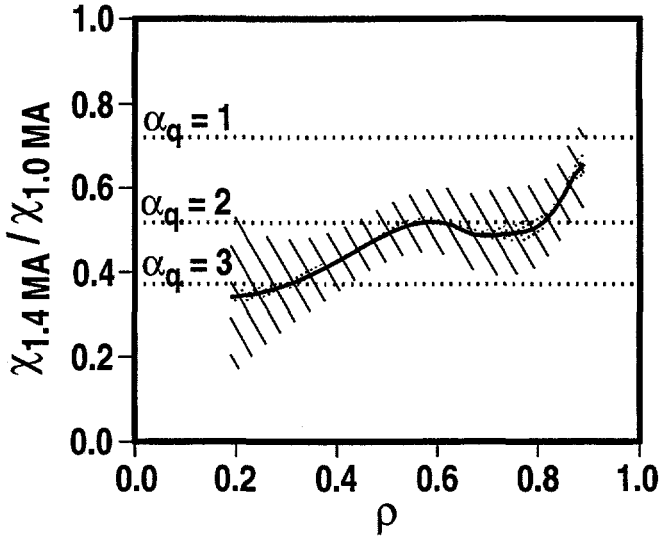

Fig. 3. Ratio of effective thermal diffusivities for the 1.4 and 1.0 MA H–mode discharges with fixed magnetic shear. The lined shading indicates the standard deviation of the random error, while the dotted shading indicates the potential effect of systematic error.

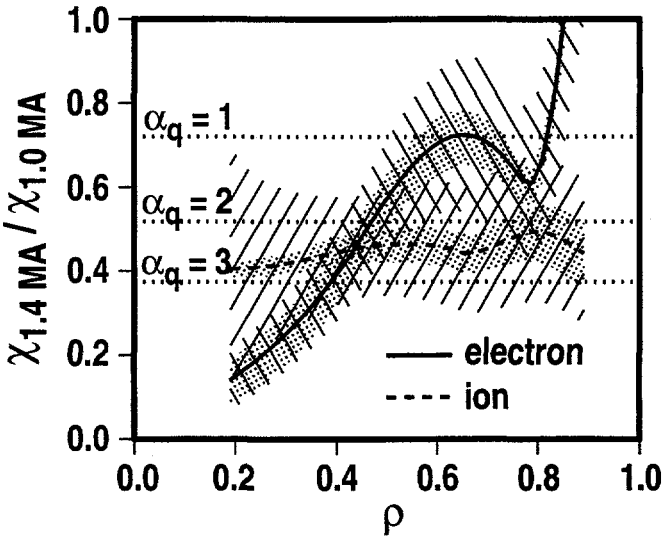

Fig. 4. Ratio of ion and electron thermal diffusivities for the 1.4 and 1.0 MA H–mode discharges with fixed magnetic shear. The lined shading indicates the standard deviation of the random error, while the dotted shading indicates the potential effect of systematic error.

energies were also matched to within 4%. The radial profiles of the safety factor and magnetic shear are shown in Fig. 5. The values of q_0 were a good match in these two discharges, and the values of q near the plasma edge scaled like the ratio of the plasma currents. As a result, the magnetic shear for the low-I discharge was an average of 40% stronger than for the high-I discharge, although this change cannot be made uniform across the plasma radius.

Table III: Physical and dimensionless parameters for H–mode safety-factor scaling experiment at fixed q_0.

Parameter	#92120	#92113
I (MA)	0.95	1.39
B (T)	1.90	1.90
R (m)	1.681	1.672
a (m)	0.611	0.605
$\bar{n}$ (10^{19} m^{-3})	4.42	4.32
W_{th} (MJ)	0.63	0.60
P (MW)	7.51	4.31
τ_{th} (s)	0.083	0.140
ε	0.36	0.36
κ	1.77	1.83
δ	0.22	0.25
q_{95}	5.52	3.85
q_0	1.2	1.2
β^{th} (%)	1.56	1.45
β_N^{th}	1.90	1.20

The change in the thermal confinement time was weaker for the combined safety factor and magnetic shear scan at fixed q_0 than for the q scan at fixed $\hat{s}$. Table III shows that the thermal confinement time increased only by 70% for a decrease in q_{95} of 30%. Therefore, the thermal confinement for H–mode plasmas scaled like $\tau_{th} \propto q_{95}^{-1.43}$ for the case of fixed q_0 [since the safety factor was not varied by a uniform amount over the plasma radius, the value of q_{95} was chosen to represent the independent variable in Eq. (2)]; the random error in the q scaling exponent is less than 0.23 while the systematic error is thought to be less than ± 0.03. The relationship of this global q_{95} scaling of confinement to the empirically-derived physical parameter scaling relations is discussed in Section V.

Although one may be tempted to conclude that the smaller variation in the thermal confinement time for the combined q and $\hat{s}$ scan in Table III, compared to the fixed $\hat{s}$ scan in Table II, was due to a magnetic shear dependence of confinement, a local transport analysis is required to properly take into account the difference in the local q profiles for these two cases. Since it was shown in Section III.A that heat transport has a strong q dependence, the change in the thermal confinement time for the fixed q_0 scan should naturally be less than the change for the fixed $\hat{s}$ scan because the change in the volume-averaged safety factor was also smaller. Before the results of the local transport analysis are discussed, it is important to verify that the local values of the plasma parameters were held constant during the combined q and $\hat{s}$ scan. The radial profiles of the electron and ion

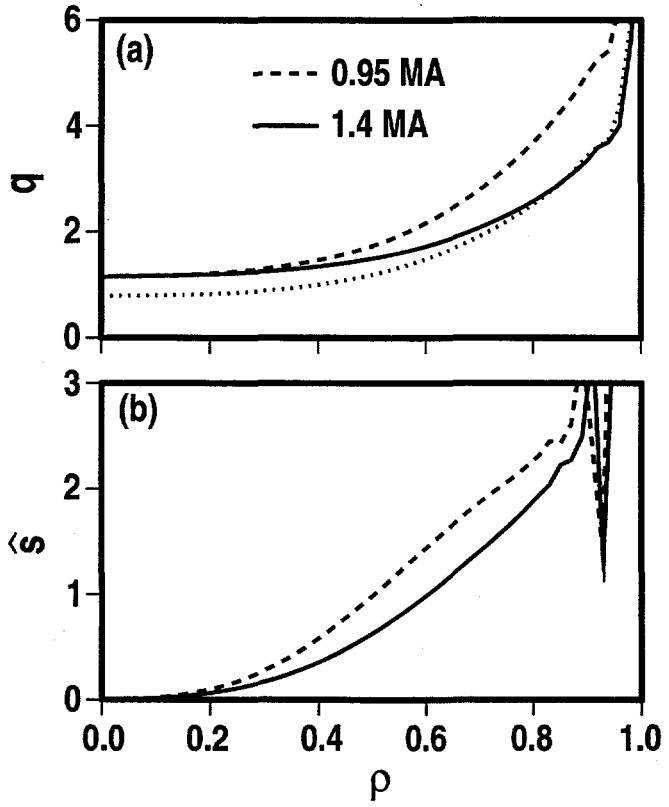

Fig. 5. Radial profiles of (a) safety factor, and (b) magnetic shear for the H–mode discharges in Table III. The dotted line in (a) represents the 0.95 MA profile scaled to 1.4 MA.

temperature, the electron density and the effective ion charge are shown in Fig. 6. The largest mismatch was again in the Z_{eff} profile; however, the other plasma profiles were well matched except for T_i near the plasma center.

A local transport analysis found that the smaller variation in the confinement for the fixed q_0 scan in Table III, compared to the fixed $\hat{s}$ scan in Table II, could more than be accounted for by the differences in the local q values and was not due to a favorable $\hat{s}$ dependence of transport. This is shown in Fig. 7, which plots the ratio of the effective thermal diffusivities given by Eq. (4) for the two H–mode discharges in Table III. The dashed line in Fig. 7 shows the expected ratio in χ_{eff} due to the experimentally-determined safety-factor scaling in Fig. 3. For the outer half of the plasma ($\rho > 0.5$), the measured change in χ_{eff} can be accounted for by the q dependence determined in Section III.A without any additional $\hat{s}$ dependence to within the experimental uncertainties. However, the theoretically expected dependence of heat transport on magnetic shear[20,22] also cannot be ruled out by this data. For the inner half of the plasma ($\rho < 0.5$), the measured change in χ_{eff} was larger than what can be accounted for by the experimentally-determined q scaling. If this difference is due to an $\hat{s}$ dependence of heat transport, then the direction of this change is such that transport is increased for increasing magnetic shear. This direction of the $\hat{s}$

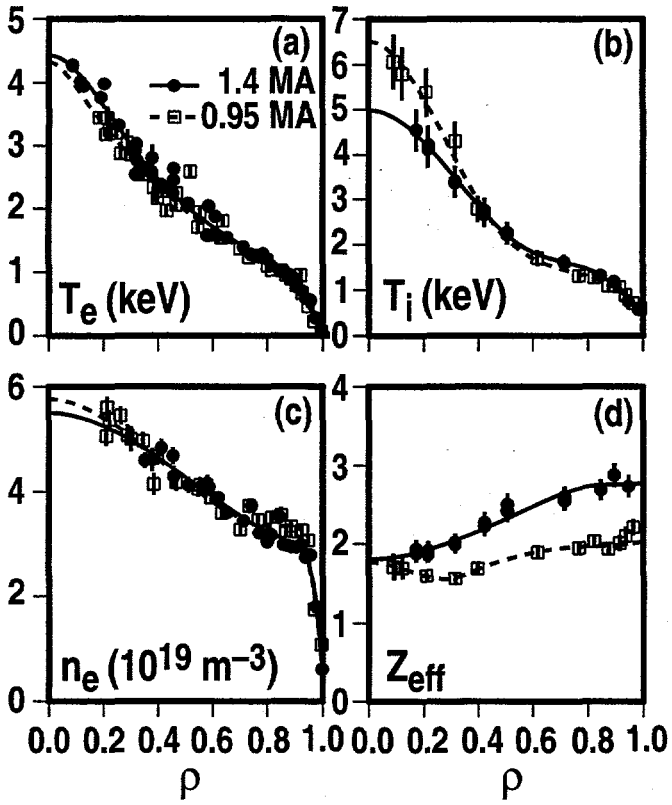

Fig. 6. Radial profiles of (a) electron temperature, (b) ion temperature, (c) electron density, and (d) effective ion charge for the H–mode discharges in Table III.

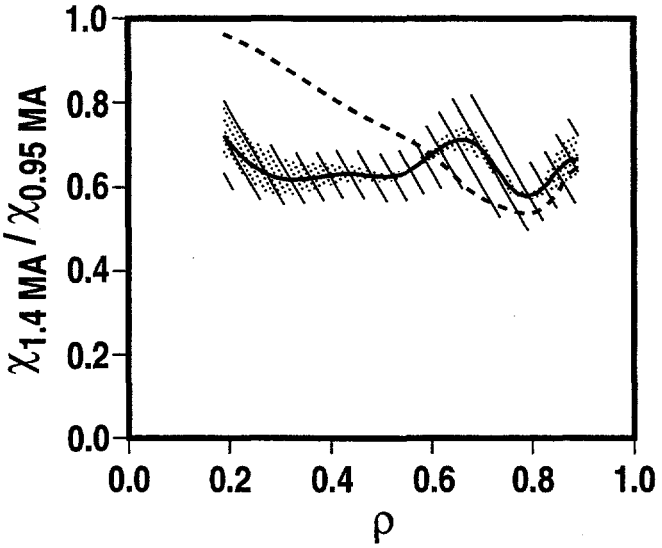

Fig. 7. Ratio of effective thermal diffusivities for the 1.4 and 0.95 MA H–mode discharges with fixed q_0. The dashed line shows the expected change in the ratio due to the measured q dependence in Fig. 3.

dependence is theoretically expected in the weak and negative shear regimes,[22] and indeed the magnetic shear was very weak near the plasma center for these discharges. However, the data in Fig. 7 would seem to indicate that the maximum of the transport dependence on magnetic shear, where the $\hat{s}$ dependence changes sign, is located around $\hat{s} \sim 1$, which is a somewhat higher value than theoretically expected.

A two-fluid transport analysis found that the apparent magnetic shear dependence of heat transport in the inner region of the plasma was due to the electron channel and not the ion channel. The ratio of the ion and electron thermal diffusivities for the combined q and $\hat{s}$ scan are shown in Fig. 8. The dashed line in Fig. 8 represents the expected ratio of the ion and electron thermal diffusivities due to the experimentally-determined safety-factor scaling in Fig. 4, handling the ion and electron fluids separately. Figure 8(a) shows that the measured change in χ_i can be completely accounted for by the q dependence determined in Section III.A for the ions. However, the measured change in χ_e shown in Fig. 8(b) was much larger than what can be explained by the experimentally-determined q scaling for electrons in the inner half of the plasma. As was the case for the effective thermal diffusivity, if this difference is due to a magnetic shear dependence, then the direction of this change is such that χ_e is increased for increasing $\hat{s}$ over the range $0 < \hat{s} < 1$.

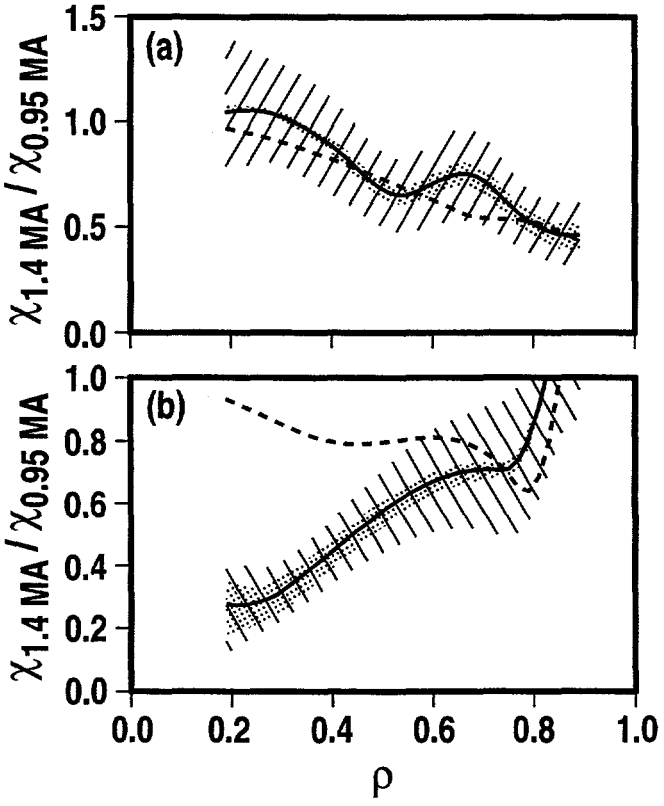

Fig. 8. Ratio of (a) ion thermal diffusivities, and (b) electron thermal diffusivities for the 1.4 and 0.95 MA H–mode discharges with fixed q_0. The dashed lines show the expected change in the ratios due to the measured q dependence in Fig. 4.

IV. Gyroradius, Beta, and Collisionality Scaling of H–mode Confinement

In this section, the results from ρ_*, β, and ν scaling experiments in H–mode plasmas on DIII–D are summarized. The implications for these measured scalings on the various proposed instability mechanisms of turbulent transport are also discussed.

Gyroradius scaling experiments on DIII–D have shown gyro-Bohm-like scaling for ITER-relevant H–mode discharges both globally and locally.[9] The scaling of heat transport with the relative gyroradius is of particular interest since ρ_* is the only dimensionless parameter that will vary significantly between present day machines and future ignition devices.[3] Traditionally, the ρ_* scaling has been interpreted as indicating the characteristic radial wavelength λ of the plasma turbulence responsible for anomalous transport, where gyro-Bohm-like scaling implies that λ is on the order of the Larmor radius and Bohm-like scaling implies that λ is on the order of the plasma radius. On DIII–D, the thermal confinement time was found to scale like $B\tau_{th} \propto \rho_*^{-3.15\pm0.2}$, while the ρ_* scaling of the ion and electron thermal diffusivities were also found to be close to gyro-Bohm-like across the plasma radius. In addition, experiments in H–mode plasmas on DIII–D have determined that the ρ_* scaling of the particle diffusivity for an helium impurity was also gyro-Bohm-like.[26] These results are consistent with the majority of anomalous transport theories that assume that the radial wavelength (or radial correlation length) of the turbulence scales with the Larmor radius.

Beta scaling experiments on DIII–D have found confinement to have only a weak beta dependence.[12] Theories for which $E \times B$ transport is dominant show little enhancement or perhaps even slight reduction in anomalous transport with increasing beta up to the ideal beta limit,[20] while transport models that invoke electromagnetic effects like magnetic flutter transport are generally expected to have a strong, unfavorable beta scaling. Beta scaling experiments for H–mode plasmas on DIII–D found the thermal confinement time to scale like $B\tau_{th} \propto \beta^{0.03\pm0.13}$. The ion fluid appeared to have a linear, favorable beta scaling while the electron fluid had no measurable beta dependence. This weak or possibly favorable beta dependence of the thermal diffusivities favors theories of anomalous transport for which $E \times B$ transport is dominant. In particular, the absence of unfavorable beta scaling strongly indicates that electromagnetic effects like magnetic flutter transport are not an important element of the turbulent transport process.

Collisionality scaling experiments on DIII–D showed a reduction in heat transport with decreasing ν for H–mode plasmas.[14] Drift wave models of anomalous transport can generally be classified by their predicted dependence on collisionality.[27] The thermal

diffusivities for collisionless ITG and collisionless trapped electron modes are expected to exhibit little dependence on ν,[20] while the thermal diffusivity for the resistive ballooning mode is predicted to increase with increasing ν.[21] Alternatively, the thermal diffusivities for the dissipative trapped electron and dissipative trapped ion modes are expected to decrease with increasing ν. Experiments on DIII–D found the heat transport to increase with increasing ν, with the thermal confinement time scaling like $B\tau_{th} \propto \nu^{-0.42\pm0.03}$ for a factor-of-8 scan in ν. A portion of this collisionality scaling could be attributed to the unfavorable ν dependence of neoclassical transport. Thus, it appears that the measured ν dependence falls somewhere between the $\chi \sim \nu^0$ dependence expected for collisionless ITG and collisionless trapped electron modes and the $\chi \sim \nu^1$ dependence predicted by collisional drift wave theories.

V. Comparison of Dimensionless and Physical Parameter Scalings

Since all of these dimensionless parameter scaling studies on DIII–D were performed in similar ELMing H–mode plasmas with an ITER-relevant plasma shape, the combined dimensionless parameter scalings can be compared to the empirically-derived physical parameter scalings developed for the ITER project. Converting a global confinement scaling relation from dimensionless variables to physical variables is a straightforward algebraic manipulation. Assuming a power law form for the scaling relation, the dimensionless parameter scalings studies for H–mode plasmas on DIII–D can be summarized as

$$B\tau_{th} \propto \rho_*^{-3.15\pm0.2}\beta^{0.03\pm0.13}\nu^{-0.42\pm0.03}q_{95}^{-1.43\pm0.23} . \quad (5)$$

Converting this dimensionless parameter scaling relation to physical parameters gives

$$\tau_{th} \propto I^{0.84\pm0.16}B^{0.39\pm0.21}n^{0.18\pm0.07}P^{-0.41\pm0.06}L^{2.00\pm0.24} , \quad (6)$$

where L represents the physical size scaling (*i.e.*, a, R, *etc.*) needed to make the scaling relation dimensionally correct. Thus it can be seen that the dimensionless parameter scaling approach yields a definitive prediction for the size scaling of confinement from single machine experiments. Equation (6) shows that the combination of four separate dimensionless parameter scans gives nearly linear current dependence, weak density scaling, and nearly square-root power degradation of confinement.

It is interesting to compare this scaling result to the global confinement scaling relations that are derived from regression analysis of multi-machine confinement databases. For example, a commonly-used thermal confinement scaling that was derived from a dataset of H–mode plasmas on DIII–D and JET is[28,29]

$$\tau_{th} \propto I^{0.9}B^{0.3}n^{0.2}P^{-0.5}L^{1.5} , \quad (7)$$

where L again represents the size scaling of confinement. Comparing Eqs. (6) and (7) finds that the I, B, and n scalings are the same, while the differences in the P and size scalings are not large enough to exclude agreement at the 2σ level. For ELM-free H–mode plasmas, a thermal confinement scaling that is nearly dimensionally correct has been determined for the ITER project,[30]

$$\tau_{ITER\text{-}93H} = 0.036 I^{1.06}B^{0.32}n_{19}^{0.17}P^{-0.67}R^{1.9}a^{-0.11}A^{0.41}\kappa^{0.66} . \quad (8)$$

A comparison of Eqs. (6) and (8) finds that the B, n, and size scalings agree to within 1σ, while the difference in the I scalings is only a little larger. The main discrepancy is in the

power scaling, where the dimensionless parameter scaling experiments on DIII–D find a much weaker power degradation than does the ITER-93H scaling relation. This discrepancy is partly due to the strong unfavorable beta dependence that is contained in Eq. (8), which was not observed experimentally.[12] This difference in the power scaling is significant because the expected heating power in ITER is ≈ 30 times that in DIII–D. Therefore, the dimensionless parameter scaling studies on DIII–D lead to an optimistic projection for H–mode confinement on larger machines.[31]

VI. Conclusions

Comparison of dimensionally identical discharges on DIII–D and JET for ELMing H–mode plasmas found that the (normalized) thermal confinement times were in good agreement. This indicates that transport is a function of the dimensionless parameters, and provides confidence on the dimensionless parameter scaling approach. Future experiments will compare the local values of the thermal diffusivities as well as the global confinement.

Experiments on DIII–D found a strong safety factor scaling of heat transport at all radii for ELMing H–mode plasmas. In the first experiment, the safety factor was varied by a factor-of-1.4 at fixed magnetic shear while the other dimensionless parameters such as ρ_*, β, and ν were kept constant. The thermal confinement time scaled like $\tau_{th} \propto q^{-2.42}$, with a random error in the q scaling exponent of less than 0.31 and a systematic error thought to be less than ± 0.03. The one-fluid thermal diffusivity exhibited the same q dependence as the global confinement, $\chi_{eff} \propto q^{2.3\pm0.64}$ with the electron and ion thermal diffusivities having the same q scaling to within the experimental errors except near the plasma edge. In the second experiment, the safety factor and magnetic shear were both varied such that q_{95} was scanned at fixed q_0. A weaker thermal confinement scaling was measured for this case, $\tau_{th} \propto q_{95}^{-1.43}$, with a random error of 0.23 and a systematic error of not more than ± 0.03 in the q scaling exponent; this weaker scaling was attributed to the smaller variation in the volume-averaged q profiles. The change in the ion thermal diffusivity for the combined q and $\hat{s}$ scan could be accounted for by the q scaling alone, although an $\hat{s}$ dependence in line with theoretical expectations could not be ruled out due to experimental uncertainties. The change in the electron thermal diffusivity was larger than could be accounted for by the q scaling alone for the inner half of the plasma. If this difference is due to the magnetic shear dependence of transport, then the direction of this change is such that χ_e is increased for increasing $\hat{s}$ over the range $0 < \hat{s} < 1$.

Combining the results of the gyroradius, beta, collisionality, and safety factor scans for H–mode plasmas on DIII–D yields a strong experimental constraint on theoretical models of turbulent transport. The dimensionless parameter scalings have been shown to reproduce the physical parameter scalings of confinement derived from regression analysis of multi-machine databases, with the possible exception of weaker power degradation. The observation of weak or possibly favorable beta scaling along with gyro-Bohm-like energy and particle transport indicates that $E \times B$ transport from drift wave turbulence is a plausible basis for anomalous transport; the experimental results are not consistent with theories for which magnetic flutter transport is dominant. The measured ν and q scalings would appear to fall part way between those of the collisionless ITG and collisionless trapped electron modes and that of the resistive ballooning mode, suggesting that for these H–mode plasmas

the actual transport process is intermediate between these two limits. The collisionality scaling of the dissipative trapped electron and dissipative trapped ion modes was not observed. In order to use these dimensionless parameter scaling experiments to further test theories of turbulent transport, the experimental profiles from these studies are in the process of being simulated using several theory-based transport models.

Acknowledgments

The authors would like to thank T.H. Osborne and J.S. deGrassie for operating the tokamak for some of these experiments.

This work is supported by the U.S. Department of Energy under Contract Nos. DE-AC03-89ER51114, W-7405-ENG-36, and DE-AC05-96OR22464.

References

[1]B.B. Kadomtsev, Sov. J. Plasma Phys. **1**, 295 (1975).

[2]J. W. Connor and J.B. Taylor, Nucl. Fusion **17**, 1047 (1977).

[3]R.E. Waltz, J.C. DeBoo, and M.N. Rosenbluth, Phys. Rev. Lett. **65**, 2390 (1990).

[4]J.P. Christiansen, P.M. Stubberfield, J.G. Cordey, C. Gormezano, C.W. Gowers, J. O'Rourke, D. Stork, A. Taroni, and C.D. Challis, Nucl. Fusion **33**, 863 (1993).

[5]F.W. Perkins, C.W. Barnes, D.W. Johnson, S.D. Scott, M.C. Zarnstorff, M.G. Bell, R.E. Bell, C.E. Bush, B. Grek, K.W. Hill, D.K. Mansfield, H. Park, A.T. Ramsey, J. Schivell, B.C. Stratton, and E. Synakowski, Phys. Fluids B **5**, 477 (1993).

[6]C.C. Petty, T.C. Luce, R.I. Pinsker, K.H. Burrell, S.C. Chiu, P. Gohil, R.A. James, and D. Wròblewski, Phys. Rev. Lett. **74**, 1763 (1995).

[7]U. Stroth, G. Kühner, H. Maassberg, H. Ringler, and the W7-AS Team, Phys. Rev. Lett. **70**, 936 (1993).

[8]J. B. Wilgen, M. Murakami, J.H. Harris, T.S. Bigelow, R.A. Dory, B.A. Carreras, S.C. Aceto, D.B. Batchelor, L.R. Baylor, G.L. Bell, J.D. Bell, R.J. Colchin, E.C. Crume, N. Dominguez, J.L. Dunlap, G.R. Dyer, A.C. England, R.F. Gandy, J.C. Glowienka, R.C. Goldfinger, R.H. Goulding, G.R. Hanson, C. Hidalgo, S. Hiroe, S.P. Hirshman, L.D. Horton, H.C. Howe, D.P. Hutchinson, R.C. Isler, T.C. Jernigan, H. Ji, H. Kaneko, L.M. Kovrizhnykh, M. Kwon, R.A. Langley, D.K. Lee, K.M. Likin, J.F. Lyon, C.H. Ma, M.M. Menon, P.K. Mioduszewski, O. Motojima, H. Okada, S. Paul, A.L. Qualls, D.A. Rasmussen, R.K. Richards, J.A. Rome, M.J. Saltmarsh, K.A. Sarksyan, M. Sato, J.G. Schwelberger, K.C. Shaing, M.G. Shats, T.D. Shepard, J.E. Simpkins, C.E. Thomas, T. Uckan, K.L. Vander Sluis, M.R. Wade, W.R. Wing, H. Yamada, and J.J. Zielinski, Phys. Fluids B **5**, 2513 (1993).

[9]C.C. Petty, T.C. Luce, K.H. Burrell, S.C. Chiu, J.S. deGrassie, C.B. Forest, P. Gohil, C.M. Greenfield, R.J. Groebner, R.W. Harvey, R.I. Pinsker, R. Prater and R.E. Waltz, Phys. Plasmas **2**, 2342 (1995).

[10]J. G. Cordey, B. Balet, D. Campbell, C.D. Challis, J.P. Christiansen, C. Gormezano, C. Gowers, D. Muir, E. Righi, G.R. Saibene, P.M. Stubberfield and K. Thomsen, Plasma Phys. Contr. Fusion **38**, A67 (1996).

[11]S.D. Scott, C.W. Barnes, D.R. Mikkelsen, F.W. Perkins, M.G. Bell, R.E. Bell, C.E. Bush, D. Ernst, E.D. Fredrickson, B. Grek, K.W. Hill, A.C. Janos, F.C. Jobes, D.W. Johnson, D.K. Mansfield, D.K. Owens, H.K. Park, S.F. Paul, A.T. Ramsey, J. Schivell, B.C. Stratton, E.J. Synakowski, W.M. Tang, and M.C. Zarnstorff, in *Plasma Physics and Controlled Nuclear Fusion Research*, Würzburg, 1992, (International Atomic Energy Agency, Vienna, 1993), Vol. 3, p 427.

[12]C.C. Petty, T.C. Luce, D.R. Baker, J.C. DeBoo, M.R. Wade, and R.E. Waltz, "Scaling of heat transport with beta in the DIII–D tokamak," submitted to Nuclear Fusion.

[13]J. G. Cordey and the JET Team, in *Plasma Physics and Controlled Nuclear Fusion Research*, Montreal, 1996 (International Atomic Energy Agency, Vienna, 1997), Vol. 1, p. 603.

[14]T.C. Luce, C.C. Petty, B. Balet, and J.G. Cordey, in P*lasma Physics and Controlled Nuclear Fusion Research*, Montreal, 1996 (International Atomic Energy Agency, Vienna, 1997), Vol. 1, p. 611.

[15]J.L. Luxon and L.G. Davis, Fusion Technol. **8**, 441 (1985).

[16]E. Bertolini, M. Huguet, and the JET Team, in *Proc. 12th Symposium on Fusion Engineering*, Monterey, 1987 (Institute of Electrical and Electronic Engineers, Piscataway, NJ, 1987), Vol. 2, p. 978.

[17]P.-H. Rebut, V. Chuyanov, M. Huguet, R. Parker, and Y. Shimomura, in *Plasma Physics and Controlled Nuclear Fusion Research*, Seville, 1994 (International Atomic Energy Agency, Vienna, 1995), Vol. 2, p. 451.

[18]J.R. Ferron, L.L. Lao, T.S. Taylor, Y.B. Kim, E.J. Strait, and D. Wròblewski, Phys. Fluids B **5**, 2532 (1993).

[19]J.W. Connor and H.R. Wilson, Plasma Phys. Contr. Fusion **36**, 719 (1994).

[20]R.E. Waltz, G.M. Staebler, W. Dorland, G.W. Hammett, M. Kotschenreuther, and J.A. Konings, Phys. Plasmas **4**, 2482 (1997).

[21]A. B. Hassam, Phys. Fluids B **4**, 1846 (1992).

[22]R.E. Waltz, G.D. Kerbel, J. Milovich, and G.W. Hammett, Phys. Plasmas **2**, 2408 (1995).

[23]B.W. Rice, T.S. Taylor, K.H. Burrell, T.A. Casper, C.B. Forest, H. Ikezi, L.L. Lao, E.A. Lazarus, M.E. Mauel, B.W. Stallard, and E.J. Strait, Plasma Phys. Contr. Fusion **38**, 869 (1996).

[24]B.W. Rice, K.H. Burrell, L.L. Lao, and Y.-R. Lin-Liu, Phys. Rev. Lett. **79**, 2694 (1997); D. Wròblewski and L.L. Lao, Rev. Sci. Instrum. **63**, 5140 (1992).

[25]H. St. John, T.S. Taylor, Y.-R. Lin-Liu, and A.D. Turnbull, in *Plasma Physics and Controlled Nuclear Fusion Research*, Seville, 1994 (International Atomic Energy Agency, Vienna, 1995), Vol. 3, p. 603.

[26]M.R. Wade, T.C. Luce, and C.C. Petty, Phys. Rev. Lett. **79**, 419 (1997).

[27]J.W. Connor, Plasma Phys. Control. Fusion **30**, 619 (1988).

[28]D.P. Schissel *et al.*, Nucl. Fusion **31**, 73 (1991).

[29]D.P. Schissel, M.A. Mahdavi, J.C. DeBoo, and M. Le, Nucl. Fusion **34**, 1401 (1994).

[30]S.M. Kaye and the ITER Joint Central Team and Home Teams, in *Plasma Physics and Controlled Nuclear Fusion Research*, Seville, 1994 (International Atomic Energy Agency, Vienna, 1995), Vol. 2, p. 525.

[31]C.C. Petty and T.C. Luce, Nucl. Fusion **37**, 1 (1997).